

Article

Evaluation of Wood Quality Traits in *Salix viminalis* Useful for Biofuels: Characterization and Method Development

Jie Gao, Mohamed Jebrane , Nasko Terziev  and Geoffrey Daniel * 

Department of Forest Biomaterials and Technology/Wood Science, Swedish University of Agricultural Sciences, P.O. Box 7008, SE-750 07 Uppsala, Sweden; jie.gao@slu.se (J.G.); mohamed.jebrane@slu.se (M.J.); nasko.terziev@slu.se (N.T.)

* Correspondence: geoffrey.daniel@slu.se

Abstract: *Salix* (willow) is a well-known coppice plant that has been used as a source for bioenergy for decades. With recent developments in changing from a fossil-based to a circular bioeconomy, greater interest has been orientated towards willow as a potential source of biomass for transport biofuels. This has created increasing interest for breeding strategies to produce interesting genotypic and phenotypic traits in different willow varieties. In the present study, 326 genetically distinct clones and several commercial varieties of *S. viminalis* were analyzed using complementary approaches including density, chemical, image, histochemical, and morphometric analyses. A systematic approach was adopted whereby the basal regions of harvested stems were separated and used in all studies to aid comparisons. Density analyses were performed on all clone individuals, and from the results, 20 individual plants representing 19 clones were selected for the more in-depth analyses (chemical, image analysis, histochemical, and morphometric). The absolute dry density of the clones selected varied between ca. 300 and 660 kg/m³ with less variation seen in the commercial *S. viminalis* varieties (ca. 450–520 kg/m³). Selected clones for chemical analysis showed the largest variation in glucose (47.3%–60.1%; i.e., cellulose) and total sugar content, which ranged between ca. 61 and 77% and only ca. 16 and 22% for lignin. Image analyses of entire basal stem sections showed presence of tension wood in variable amounts (ca. 7%–39%) with characteristic G-fibers containing cellulose-rich and non-lignified gelatinous layers. Several of the clones showing prominent tension wood also showed high glucose and total sugar content as well as low lignin levels. A morphometric approach using an optical fiber analyzer (OFA) for analyzing 1000 s (minimum 100,000 particles) of macerated fibers was evaluated as a convenient tool for determining the presence of tension wood in stem samples. Statistical analyses showed that for *S. viminalis* stems of the same density and thickness, the OFA approach could separate tension wood fibers from normal wood fibers by length but not fiber width. Results emphasized considerable variability between the clones in the physical and chemical approaches adopted, but that a common aspect for all clones was the occurrence of tension wood. Since tension wood with G-fibers and cellulose-rich G-layers represents an increased source of readily available non-recalcitrant cellulose for biofuels, *S. viminalis* breeding programs should be orientated towards determining factors for its enhancement.

Keywords: *Salix viminalis* L.; bioenergy crops; lignocellulose biofuels; biomass recalcitrance; plant breeding



Citation: Gao, J.; Jebrane, M.; Terziev, N.; Daniel, G. Evaluation of Wood Quality Traits in *Salix viminalis* Useful for Biofuels: Characterization and Method Development. *Forests* **2021**, *12*, 1048. <https://doi.org/10.3390/f12081048>

Academic Editor: František Kačík

Received: 4 June 2021

Accepted: 4 August 2021

Published: 6 August 2021

Publisher's Note: MDPI stays neutral with regard to jurisdictional claims in published maps and institutional affiliations.



Copyright: © 2021 by the authors. Licensee MDPI, Basel, Switzerland. This article is an open access article distributed under the terms and conditions of the Creative Commons Attribution (CC BY) license (<https://creativecommons.org/licenses/by/4.0/>).

1. Introduction

Recent developments in society for changing from a fossil-based to a circular bioeconomy has created greater interest for using short-rotation coppice plants (e.g., willow) as a potential biomass source for transport biofuels such as bioethanol and biogas [1–7]. The use of bioenergy is ever increasing having grown by 150% since 2000 in the EU, while the use of biofuels in transport is up 25-fold; thus, there is a great surge after biomass raw materials of which coppice plants are expected to provide an important part [8]. Previously, willows have been used primarily as dedicated energy crops for burning. However, it

is now realized that the short rotation system and rapid growth of coppice plants can also provide great potential as a biorefinery feedstock. In addition, coppice plants are not competitors for the human food chain, since they can be grown on land unsuitable for food or feed production. This has created an increasing need for breeding strategies for selecting important genotypic and phenotypic traits for biofuels and knowledge on how these can improve the growth and development of coppice plants such as willow (*Salix* spp.) under changing climate and agricultural situations [9,10]. *Salix* spp. lend themselves readily to breeding without genetic modification using recurrent selection. They are easily hybridized, are readily propagated through cuttings, and harbor considerable inter- and intraspecific variability [11,12]. Apart from obvious traits such as high yield and good growth on barren ground, knowledge on the fundamental stem composition and wood anatomy of different genetic *Salix* clones is also important with respect to biofuels, as these features can provide diagnostic traits (i.e., markers) useful for clone characterization. However, apart from the analysis of general traits (e.g., yield), it is not always straight forward to find representative features of analysis that may be used on large and differing plant populations grown under variable conditions in different plantations [10,13,14].

While the total stem yield (i.e., not foliage) of biomass per hectare/year is controlled by genetic and phenotypic expression and local growing conditions at a particular site, such knowledge does not give any information on the composition and chemistry of the wood material or ease for comminution and enzymatic hydrolysis. For example, for biofuel potential, both the total amount and accessible cellulose is a very important trait, while knowledge on lignin type (syringyl vs. guaiacyl lignin), and concentration at different structural levels is important for understanding biomass recalcitrance, which is possibly the most important attribute to overcome processes involving enzymatic hydrolysis [15–22]. Cellulose is the main source of glucose for hydrolysis and ethanol production potential, and lignin is the cellular basis for wood cell wall and biomass recalcitrance (i.e., inhibition to enzymatic hydrolysis). Recent studies have, for example, shown wide variations in *Salix* clone recalcitrance after dilute acid pretreatment with a threefold difference between potential ethanol yields (liter/hectare) for best and worst performing *Salix* clones in biorefining studies [13]. Similarly, with hot-water extractions, *Salix* clones have shown wide differences in sugar yields and subsequent ethanol potential [23]. At wood tissue and cellular levels, recalcitrance and density can also be greatly influenced by the presence and total amount of abnormal wood developed (e.g., tension wood, TW) [24,25]. This is because tension wood tissues are characterized by the presence of gelatinous fibers (G-fibers) with high cellulose levels and different cellular morphologies and chemical characteristics than normal fibers [24,26–29].

In the present study, we used a systematic approach to examine 326 clones from a population of genetically distinct individuals derived from a population of *S. viminalis* accessions collected previously from the wild throughout [26] Europe and Russia and vegetatively propagated [10,12]. *S. viminalis* is one of the most common *Salix* spp. used for breeding studies because of its great biomass production over rather short periods of time [11,30].

We adopted a progressive multiscale approach of analysis. Initially, all *S. viminalis* clones were examined for density as an appraisal of biomass. From these analyses, a number of clones were selected (i.e., 19) showing a range in density (i.e., low to high densities) values. Since variations in wood density are reflected by variations in wood anatomy and biomass content, detailed analyses were conducted to explain the differences. These analyses included wet chemistry to determine the total carbohydrates (i.e., cellulose, hemicelluloses) and lignin present, physical and image analyses to determine the relative growth ring proportions in stems and presence of abnormal wood (i.e., tension wood), and histochemical analyses on the micro-distribution of lignin types. Finally, fiber morphometric analyses were performed on a selection of the *S. viminalis* clones showing tension wood to determine whether its presence could be measured and used as a distinguishing feature (marker) for biofuel potential through increased and readily available cellulose. A

number of commercial *S. viminalis* clones were also included in the studies. To aid direct comparisons, all analyses were conducted on clones of the same age with samples taken from similar basal stem regions.

2. Materials and Methods

2.1. Plant Materials Harvesting and Sample Preparation

Common osier (*Salix viminalis* L.) plants were harvested during winter 2017. The plants came from a previously established population, consisting of 326 genetically distinct individuals (i.e., accessions), collected from natural standings in the wild in Europe and Russia and vegetatively cloned, planted in a completely randomized block design near Pustnäs, Uppsala, Sweden (59°49' N, 17°40' E) [12]. In the present study, the 326 clones (and replicates) consisting of 2-year-old shoots were selected from four experimental blocks. The field experiment was established in 2009. Complete details of the population have been reported previously in earlier publications by Hallingbäck et al. [10] and Berlin et al. [12].

The number of stems and fresh weight was recorded for each plant in the study, the tallest shoot of each plant was selected, and fresh weight and diameter of the shoot measured (results reported elsewhere; [31]). From each individual shoot, a ca. 25 cm-long piece from the bottom part of the shoot was cut and divided into two samples (Figure 1). The bottom part (ca. 20 cm long) was used for histochemical (image analysis) and morphometric analyses, while the upper part (ca. 5 cm long) was used for density and chemical measurements. In total, 1172 samples from the clones (ca. 3–4 biological replicates/clone) were used for density and chemical measurements (see below). In addition, two older *S. viminalis* clones and four commercial varieties were collected from a field trial originally established May 2011 in Uppsala (58°81' N, 17°66' E) on postglacial heavy clay soil. The shoots were harvested during winter 2017 when they were 2 years old.

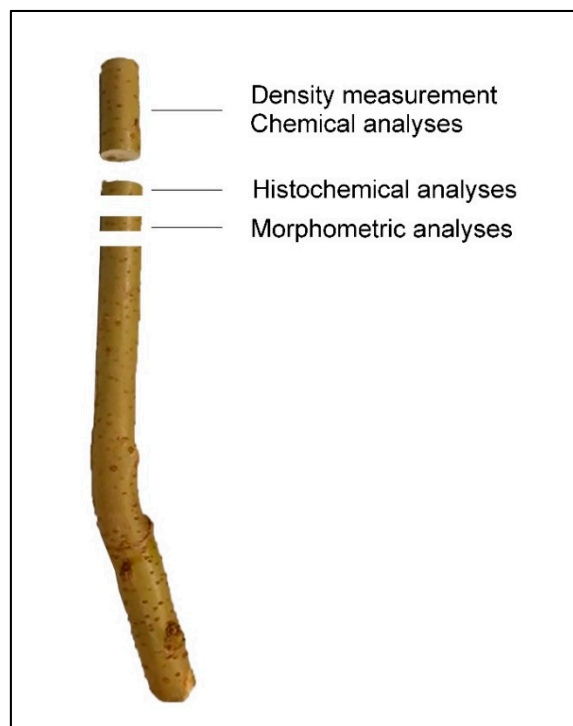


Figure 1. Overview of sampling from the basal regions of the *S. viminalis* stems.

2.2. Density Measurements

For determination of wood density (ρ), *S. viminalis* samples (ca. 5 cm long) were debarked and dried overnight in an oven at 103 ± 2 °C. After drying, the absolute dry weight of the sample was recorded, and immediately, the sample's absolute dry volume

was measured by the water displacement method [32]. The absolute dry density (ρ) of wood was determined as the mass (i.e., dry wt.) divided by volume and given in kg/m^3 . The density (ρ) of each wood sample was calculated by the average of two measurements. Variations in density measurements are expressed with respect to block variations, as individual plant values and as clonal average values across blocks. Density values were used for the selection of a range of clones/individuals (i.e., 20 plant individuals representing 19 clones) over the entire spectrum of densities for subsequent chemical, image analysis, and morphometric analyses.

2.3. Chemical Analyses

For chemical analyses, debarked samples were chipped and milled using a Retsch SM100 mill to pass a 40-mesh (0.4 mm) screen and the powder stored in airtight antistatic bags. Samples were analyzed for acid-soluble lignin (ASL), acid-insoluble lignin (AIL), and monosaccharides according to [33]. ASL was determined using a Hitachi U-2910 spectrophotometer (Hitachi, Tokyo, Japan) with an absorptivity of 110 $\text{L}/\text{g}/\text{cm}$ at a wavelength of 205 nm. Monomeric carbohydrates were determined using a Chromaster high-performance chromatography (HPLC; Hitachi, Tokyo, Japan) system equipped with an evaporative light scattering detector (ELSD-90; VWR International GmbH, Darmstadt, Germany) and a Metacarb 87P column (300 mm \times 6.5 mm; Santa Clara, CA, USA) with a guard column (Metacarb 87P 50 mm \times 4.6 mm). ELSD-90 was operated at 50 °C, 2.5 bars, and N_2 was used as the nebulizing gas. The sugars were eluted using ultrapure water as a mobile phase at a constant flow rate of 0.5 mL/min and column temperature of 85 °C. Three *S. viminalis* samples were not debarked in order to determine the effect of bark on the analyses. Chemical results were determined as the average of 3 technical replicate analyses made on 300 mg *Salix* clone wood taken from each of the milled 5 cm stem samples (Figure 1).

2.4. Analysis of Growth Ring Proportions and Presence of Tension Wood

Entire stem cross-sections (ca. 15–30 μm thick) were cut from basal stem samples (Figure 1) using a sledge sliding microtome (Leica 1300 sledge microtome). Sections were double-stained with 1% *w/v* chlorazol black E and 0.1% *w/v* safranin to visualize the presence of tension wood (TW) [34]. Chlorazol black E strongly stains the gelatinous layer (G-layer) of TW fibers black with our previous studies showing the combination of safranin and chlorazol black E giving the best staining for image analysis [35]. Entire stem cross-sections were stained and scanned using an Epson Perfection Pro 750 film scanner with a pixel resolution of 2400 dpi and areas of TW marked. Thereafter, using Adobe Photoshop CC 2017, the pixel values of the selected TW area and the whole section area were determined. The percentage area of TW in entire stem cross-sections was then quantified using the equation: area of TW in pixels/area of the whole section in pixels \times 100%.

Presence of tension wood regions and fibers with gelatinous layer (i.e., G-fibers) after staining was confirmed using a Leica DMLB light microscope (Leica Microsystems, Wetzlar, Germany) equipped with an Infinity X-32 digital camera (Deltapix, Samourn, Denmark). To visualize lignin distributions, fresh sections were stained using the Wiesner and Mäule reactions [36,37]. For the Wiesner reaction, sections were treated with 2% *v/v* phloroglucinol in ethanol and mounted in 6 M hydrochloric acid. For the Mäule reaction, sections were stained with 1% *w/v* potassium permanganate for 5 min, washed (5 min in water), treated with 2 M HCl for 5 min, washed (5 min in water), and mounted in ammonium hydroxide. Sections were observed directly after Wiesner and Mäule reactions, as the color reaction is unstable. All stains were purchased from Sigma-Aldrich (St. Louis, MO, USA). Additional sections were stained with 1% *w/v* astra blue [35] or processed for scanning electron microscopy (SEM; [38]) for morphological observations and measurements on G-layer thickness.

2.5. Morphometric Analyses

From the chemical and image analysis studies, a number of genetically distinct *S. viminalis* clones (8), older clones (2), and commercial varieties (4) were selected for morphometric analyses of fiber characteristics including the fiber length and the width of whole *S. viminalis* wood samples and selected tension wood samples and vessel frequency. Stem pieces (ca. 1 cm³; Figure 1) were debarked by hand using a razor blade, and the pith (i.e., ca. 2–4 mm in diameter) was removed. Samples were delignified in a 1:1 mixture of 100% acetic acid and H₂O₂ at 60 °C overnight [35,39]. Following delignification, samples were washed (5 × distilled water) and macerated by agitation for 2 h, thus forming a fiber suspension for morphological analysis of cellular elements. Approximately 0.1 g dry wt. was used in ca. 1 dl distilled water for morphological analysis using an Optical fiber analyzer (OFA) (L & W FiberTester Plus; ABB AB/Lorentzen & Wettre Products, Kista, Sweden). Analyses were duplicated for each same sample. Analyses were restricted to determining variations in length-weighted (LW) fiber length and width for wood samples and regions cut out showing pronounced tension wood and the ratio of vessel frequency in TW and opposite (OW) wood. The length weighted (LW) fiber length and width is a measure that is used for analysis of fiber populations during pulp and paper manufacture, where variations in fiber length and width can vary significantly during secondary refining of fibers during mechanical and chemical pulping. Results are given as total fiber length or width in per mille (‰). A minimum of 100,000 fibers (i.e., particles) were analyzed per sample. Pearson's correlation analysis was used to determine differences in fiber analysis and correlation with stem density. For comparison, in one example, the vessel frequency determined using the OFA was compared with direct quantification (i.e., counting) of vessel frequency in semi-thin stem sections of *S. viminalis* clone 81041 TW and OW using scanning electron microscopy (SEM). *S. viminalis* sections were cut and prepared for SEM as previously described [35].

3. Results

3.1. Density

Results for *S. viminalis* clone density (kg/m³) measurements are shown as raw data for all individual plants of the 326 clones (i.e., in total 1172 plants) (Figure 2A), for the selected 20 plants representing 19 clones, two older clones (78183, 78195) and commercial varieties (Björn, Jorr, Olof, Tora) chosen for detailed analyses (Figure 2B, red symbols), density with respect to block origin (Figure 2C), and as raw data and average density values (Figure 2D). The absolute dry density (kg/m³) of the 1172 individual clonal plants varied between 305 and 662 kg/m³ (Figure 2A). The density of individual experimental clone replicates varied depending on block origin with block 1 giving average total densities that were slightly higher than blocks 2, 3, and 6 (Figure 2C), despite all blocks being located at the same site. The highest value of mean densities was recorded for clones 685, IA155, 43_CZ, and 67_CZ and the lowest densities for 102_PL, 738, 1293, and P86. This density range is consistent with previous reports in the literature for *S. viminalis* [40]. Less variation was observed for the *S. viminalis* commercial varieties (Figure 2B, far right), which ranged between ca. 457 and 520 kg/m³. The largest variation seen for an individual was clone 102_PL (ca. 165 kg/m³), while for the majority of the clones, the difference was ca. 19–77 kg/m³ (Figure 2B). The range of densities selected for further analysis ranged from 441 and 662 kg/m³, representing a ca. 33% difference between the lowest and highest density. A comparison of clonal average density results with the individual density values for all plants of the different clones showed a clear difference, which is indicative that both low- and high-density values of plants due to environmental causes could be easily missed (Figure 2D). Since differences in density (ca. 220 kg/m³) can normally be explained by variations in the cellular structure, anatomy, and chemistry of the wood material, further studies were aimed at looking for trends and likely reasons for the density differences.

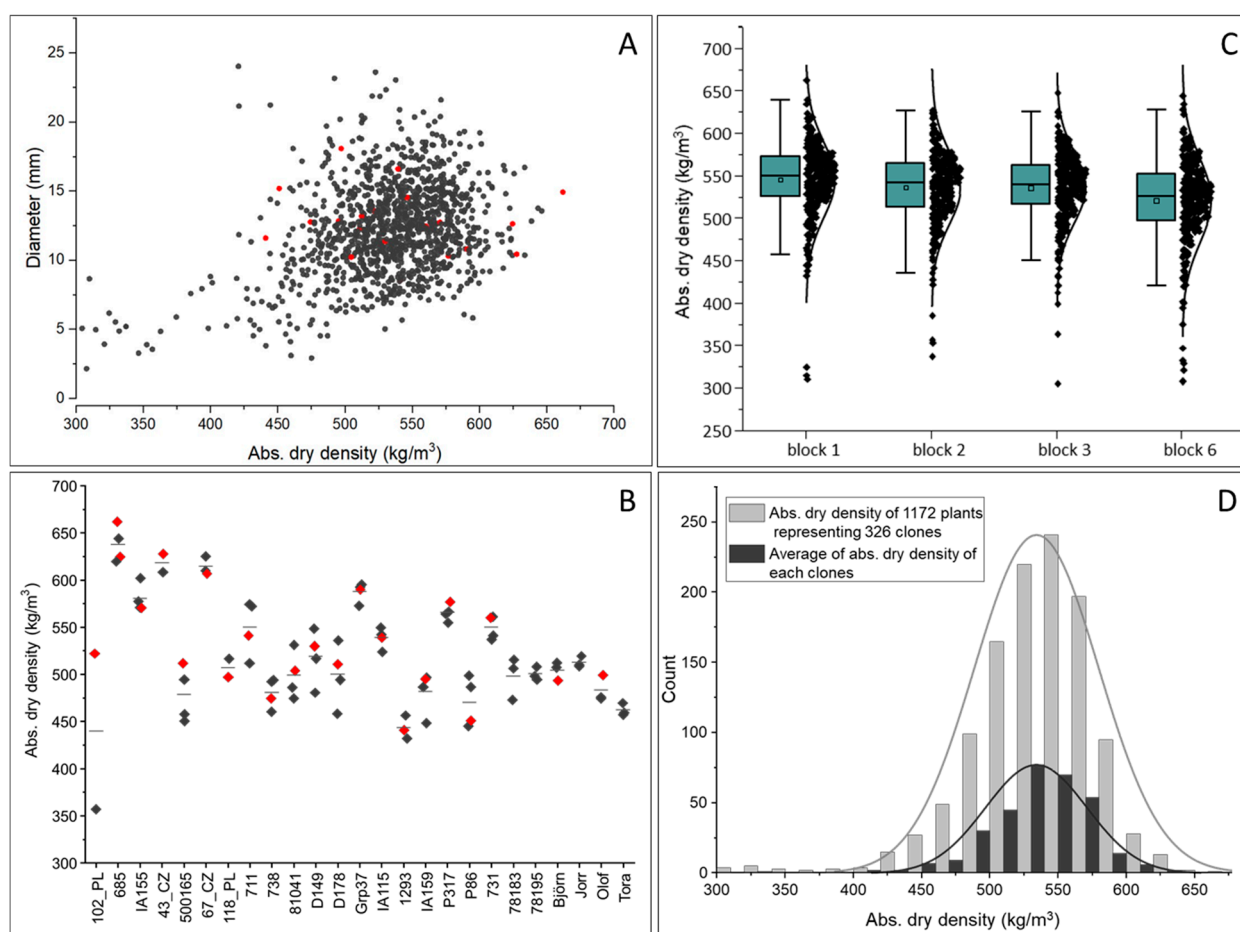


Figure 2. Absolute dry weight density (Abs. dry density) measurements for the 326 genetically distinct *S. viminalis* clones and commercial varieties. **(A)** Scatterplot of the 326 clones and replicates. Red dots indicate replicates selected for further studies; **(B)** selected genetic and commercial clones; **(C)** density distribution variations with different blocks; **(D)** density plotted as individual and average values.

3.2. Chemical Analyses

To aid comparisons, results from the wet chemical analysis for selected *S. viminalis* individuals (i.e., 20) are shown together with the % tension wood and density (kg/m³) in Table 1. Wet chemical analysis of stems showed that the total lignin (i.e., acid-insoluble and -soluble lignin) ranged by 5.6% from 16.4 (685¹: clone 685 from block 1) to 22% (711) for debarked samples. The acid-insoluble lignin (i.e., Kraft lignin) varied between 13.9% (685¹) and 20.3% (711) representing ca. 85% and 92% of the total lignin, respectively, in the debarked samples. The acid-soluble lignin varied maximally between 7.7% (clone 711) and ca. 15% of the total lignin (clone 685¹).

Table 1. Tension (%), density, and chemical analysis of sugars and lignin in selected clone samples. Chemical results reflect the average of 3 technical replicate analyses from 300 mg *S. viminalis* clone taken from milled 5 cm stem samples.

Debarked <i>S. viminalis</i> Samples	Density (kg/m ³)	Tension(%)	Lignin(%)			Carbohydrate (%)				
			AIL	ASL	Total Lignin	Glucose	Xylose	Galactose	Mannose	Total Sugar
1293	441.0	10.5	16.0	2.4	18.4	47.3	12.6	0.5	4.0	64.4
P86	451.1	20.8	18.4	2.1	20.5	52.5	11.0	0.4	2.2	66.1
738	474.3	13.6	16.0	2.0	18.0	53.1	11.2	0.4	1.2	66.0
IA159	495.2	6.9	16.2	2.4	18.6	47.8	12.7	0.4	1.9	62.8
118_PL	497.3	16.8	17.8	1.9	19.7	55.9	11.9	0.4	1.8	70.0
81041	504.1	31.1	15.1	2.2	17.3	58.6	8.4	0.4	1.9	69.3
D178	510.9	23.2	19.9	1.8	21.7	48.9	9.4	0.4	2.3	61.0
500165	512.0	15.5	16.2	2.6	18.9	51.8	10.1	0.4	1.6	63.9
102_PL	522.0	39.2	16.1	2.1	18.2	60.1	7.9	0.5	1.9	70.4
D149	529.9	11.8	16.6	2.5	19.0	52.2	12.0	0.4	2.9	67.6
IA115	539.4	21.6	16.8	2.5	19.3	54.3	12.1	0.4	1.5	68.3
711	541.3	10.8	20.3	1.7	22.0	51.3	11.2	0.4	1.9	64.8
67_CZ	548.5	20.1	19.5	1.8	21.3	49.9	10.9	0.4	1.7	62.8
731	560.2	7.6	18.5	2.4	20.9	49.3	10.3	0.4	1.7	61.8
IA155	570.7	18.4	14.9	2.4	17.3	53.6	9.2	0.5	2.8	66.1
P317	576.8	25.6	17.3	2.4	19.7	51.6	10.4	0.4	2.0	64.4
Grp37	590.2	20.5	18.9	1.9	20.8	49.4	9.7	0.4	1.9	61.4
685 ²	624.6	24.6	15.4	2.6	17.9	49.9	11.3	0.9	3.4	65.5
43_CZ	627.7	20.2	18.9	2.2	21.1	51.8	9.9	0.4	1.6	63.8
685 ¹	662.0	38.1	13.9	2.5	16.4	59.0	16.3	0.0	1.8	77.2

685²: clone 685 from block 2; 685¹: clone 685 from block 1.

The total sugar (i.e., as total carbohydrates) ranged by 16.2% from 61 (D178) to 77.2% (685¹) with glucose (i.e., cellulose) representing the major sugar with lesser amounts of xylose > mannose and > galactose. Glucose and xylose composed between 93.0% and 97.5% of the total sugars in the selected clone samples with mannose forming between 1.8% and maximally 6.2% of the total sugar (Table 1). Galactose was found at levels ranging from 0.0%–0.9% in the clone samples. Cellobiose and arabinose was not detectable in any of the debarked samples. Detection of the 6C sugar monomer is interesting as galactose is frequently associated with the presence of reaction wood (i.e., tension wood) that was present in all the *S. viminalis* clone stem cross-sections examined (see below).

The Pearson *r* (*p*-value) was used to evaluate any correlation between percent total lignin and sugars, tension area (%), and density (Table 2). Results showed moderate and strong positive correlations between tension wood, density, and total sugars and a negative correlation with lignin. Thus, an increase in the presence of tension wood provides more biomass (i.e., density), since tension wood fibers have thicker secondary cell walls with G-layers than normal wood fibers (see below). Similarly, the increase in sugar related primarily to greater amounts of glucose (cellulose) present is likely derived from G-fiber gelatinous layers. A negative correlation between tension area and lignin is expected, since on a comparative basis, the presence of more tension wood and sugar will result in a decrease in the total lignin to total sugar ratio, even if the lignin concentration remains the same.

r: Pearson correlation coefficient; $0 < |r| < 0.3$, weak correlation; $0.3 < |r| < 0.6$, moderate correlation; $0.6 < |r| < 1.0$, strong correlation.

For comparison, chemical analyses were also made on three *S. viminalis* clone samples (i.e., 1293_WB (WB = with bark); 102_PL_WB; 685¹_WB) in which the bark was retained. Essentially, similar results to debarked samples were obtained apart from sample 1293_WB, which showed higher total lignin (i.e., 23.6% vs. 18.4%) caused by higher % AIL (21.63% vs. 16.0%). All three barked clone samples showed a between 0.9% and 9.2% decrease in glucose and a between 0.27% and 5.05% decrease in xylose content (results not shown). Results suggest, however, that gross chemical analysis of barked and debarked *S. viminalis* clone

samples will likely show different results. Analysis showed that both bark thickness and morphological appearance differed significantly between the samples (results not shown).

Table 2. Pearson r (p -value) for correlation between tension area, density, total lignin, and sugars.

Debarked <i>S. viminalis</i> Samples	Tension Area (%)	Density (kg/m ³)	Total Lignin (%)	Total Sugar (%)
Tension area (%)	1	0.395 *	−0.463 **	0.622 ***
	–	(0.085)	(0.040)	(0.003)
Density (kg/m ³)		1	−0.080	0.219
		–	(0.737)	(0.353)
Total lignin (%)			1	−0.657 ***
			–	(0.002)
Total sugar (%)				1
				–

*** $p < 0.01$; ** $0.01 < p < 0.05$; * $0.05 < p < 0.1$.

3.3. Analysis and Staining of Stem Cross-Sections for Growth Rings and Presence of Tension Wood

Some physical features of selected clone stems at the basal point, including total stem diameter and percentage area occupied by the central pith and by first and second growth rings, are given in Table 3. The two-year-old debarked stems varied in thickness from ca. 8.6 to 15.2 mm (Table 3). A considerable difference was noted in stem diameter between the thinnest (8.6 mm; clone 711) and thickest stem (18.1 mm; clone 118_PL). Similarly, the pith varied between 1.7 mm (clone 118_PL) and 9.1 mm (clone 738), while the contributions of the first and second growth rings varied between 17.3% and 37.0% (clones 118_PL vs. 685¹) and 58.1% and 81.0% (clones 738 vs. 118_PL), respectively.

Table 3. Selected *S. viminalis* clones characteristics.

Debarked <i>S. viminalis</i> Samples	Stem Diameter (mm)	Pith (%)	1st Growth Ring (%)	2nd Growth Ring (%)	Tension (%)	Density (kg/m ³)
1293	11.6	3.5	19.3	77.2	10.5	441.0
P86	15.2	3.6	23.9	72.6	20.8	451.1
738	12.8	9.1	32.8	58.1	13.6	474.3
IA159	12.8	5.3	21.7	73.0	6.9	495.2
118_PL	18.1	1.7	17.3	81.0	16.8	497.3
81041	10.2	2.4	36.8	60.9	31.1	504.1
D178	12.3	3.7	18.1	78.2	23.2	510.9
500165	13.8	3.7	26.8	69.5	15.5	512.0
102_PL	13.6	2.3	22.9	74.8	39.2	522.0
D149	11.4	5.1	31.3	63.6	11.8	529.9
IA115	16.6	3.6	30.3	66.1	21.6	539.4
711	8.6	8.0	29.0	63.0	10.8	541.3
67_CZ	10.9	4.9	24.3	70.8	20.1	548.5
731	12.5	5.3	32.6	62.2	7.6	560.2
IA155	12.7	3.0	29.8	67.2	18.4	570.7
P317	10.3	4.3	20.1	75.6	25.6	576.8
Grp37	10.3	6.5	27.8	65.7	20.5	590.2
685 ²	12.6	4.4	37.0	58.5	24.6	624.6
43_CZ	10.4	4.2	26.1	69.7	20.2	627.7
685 ¹	14.9	4.1	27.3	68.5	38.1	662.0

685²: clone 685 from block 2; 685¹: clone 685 from block 1.

Analysis of stem cross-sections of selected clone samples after double staining with chlorazol black E and safranin highlighted the presence of tension wood in all stems examined (Figure 3). Light microscopy confirmed the tension wood bands and presence of wood fibers with G-layers (G-fibers). Isolated G-fibers were also distributed in the ground tissue of all the clones but were not quantified. Tension wood was characterized by the

presence of discrete black staining bands often present in both the first and second growth rings (Figure 3). Bands were not proportional to the first or second growth ring thickness of the two-year stems, and both multilateral and unilateral distributions were apparent (e.g., clone 1293 vs. 43_CZ). The presence of tension wood is normally characterized by the unilateral growth of abnormal wood (i.e., reaction wood) tissues on the upper side of the branches of hardwoods such as *Salix*. (e.g., Figure 3; clones IA115, 685¹, IA155), emphasizing that growth in the fast growing clones likely has different physiological induction parameters. Using a combination of double staining and image analysis, the area of tension wood in stem sections was quantified (Table 1, Figure 3). The greatest area percentage of tension wood in stem cross-sections was found for clone sample 102_PL with 39.2% (stem diameter 13.6 mm), and the lowest was 6.9% for clone sample IA159 (stem diameter 12.8 mm) (Table 1). Thus, despite having similar stem diameter (13.6 vs. 12.8 mm), the percentage area with tension wood was ca. 5x greater, indicating differences between the clones. A further difference between the two clone samples was the percentage pith area being ca. 2x greater in IA159 than 102_PL (i.e., 5.3 vs. 2.3; Table 1), the clone with the smaller diameter having the greater pith area. Little difference was noted between the percentage area for the first and second growth rings that were 21.7 and 22.9 and 73.0% and 74.8%, respectively, for IA159 and 102_PL. In addition, no major differences were observed in densities (495.2 vs. 522.0 kg/m³) between samples from IA159 and 102_PL (Table 1).

Light microscopy observations confirmed the presence of typical tension wood fibers (G-fibers) with pronounced gelatinous layers (Figure 4A–D). As reported previously, the G-layers appeared weakly attached to the outer secondary cell wall layer in tension fibers (i.e., S2 layer) and, after sectioning, were frequently detached (Figure 4D arrows; [35,41]). Observations of tension wood bands showed variability in the thickness of the G-layer depending on presence in earlywood (EW)/latewood (LW) and between clone samples (Figure 4E,F). Typical thickness of the G-layer in early- and latewood was of the order 0.72 (EW) to 1.85 (LW) μm , respectively (results not shown). Although quantification was not conducted, clone samples showing high glucose content (i.e., cellulose) also had pronounced tension wood (e.g., clone 102_PL: 39.2% TW; 60.1% glucose; clone 685¹: 38.1% TW; 59.0% glucose) (Table 1). Similarly, clone samples with the highest lignin tended to have lower tension wood (e.g., clone D178: 23.2% TW, 21.7% lignin; clone 711: 10.8% TW, 22.0% lignin) (Table 1), although the trend was less distinct possibly because the variation in total lignin (i.e., 5.8%) was much less than that observed for glucose (cellulose) (i.e., 12.8%). Histochemical staining showed similar variations in the micro-distribution of lignin across the clone samples. Typically, the vessels, ray parenchyma, and middle lamella regions stained more strongly for guaiacyl lignin (i.e., cinnamaldehyde groups), and the outer fiber secondary walls (i.e., S2, not G-layers) and middle lamella regions stained more strongly for syringyl lignin units (Figure 4A vs. Figure 4B,C) [35]. It was not possible using a histochemical approach for lignin to separate the clones with respect to the wet chemical analysis of lignin.

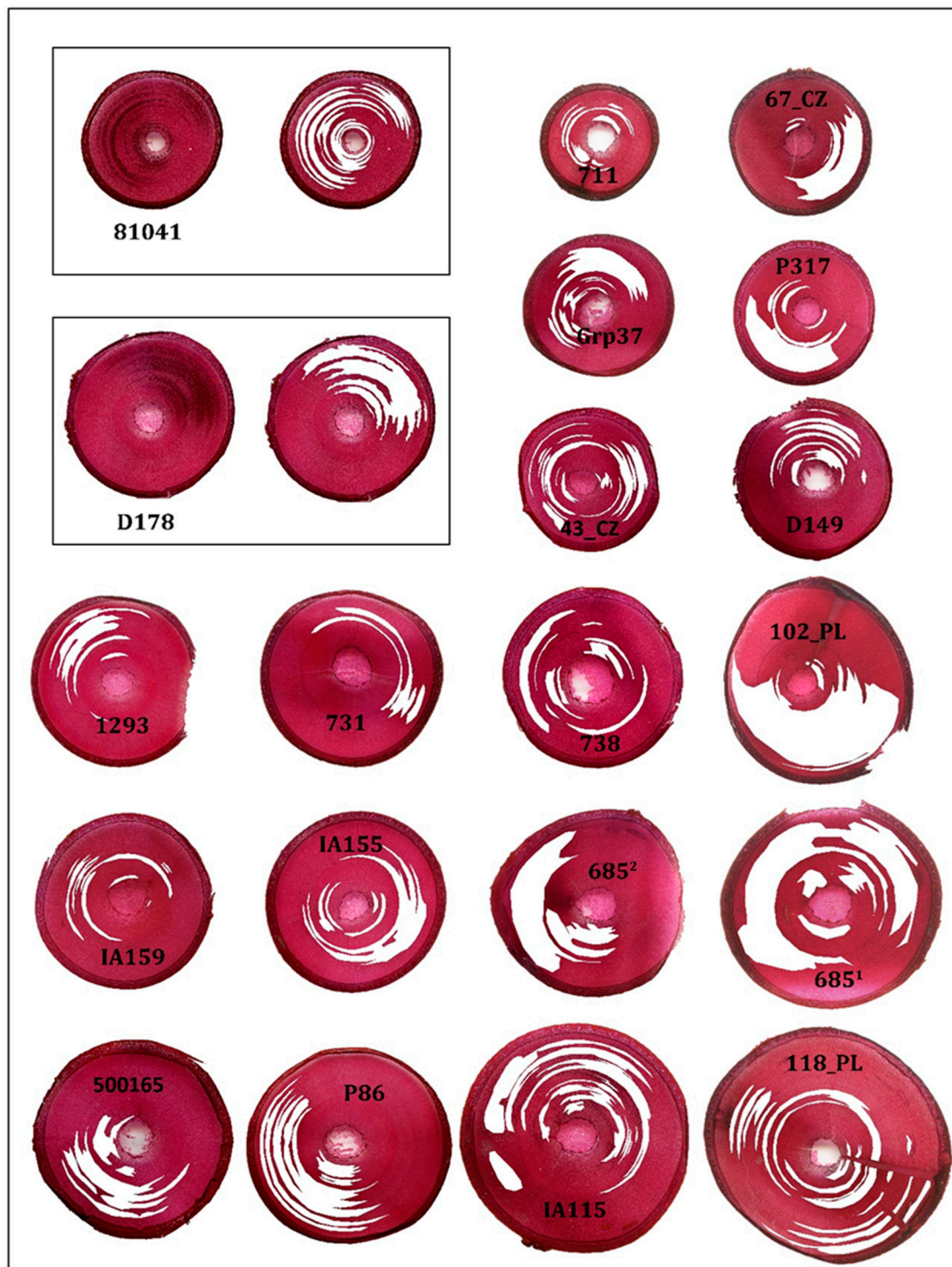


Figure 3. Images of *S. viminalis* stem basal cross-sections after double staining with chlorazol black E and safranin. Inset shows two clones with areas of tension wood before and after marking the tension wood using photoshop. The remainder of the figure shows selected clones with areas of tension wood marked only. Note that the tension wood shows variable multilateral and unilateral development in the growth rings of the two-year stems.

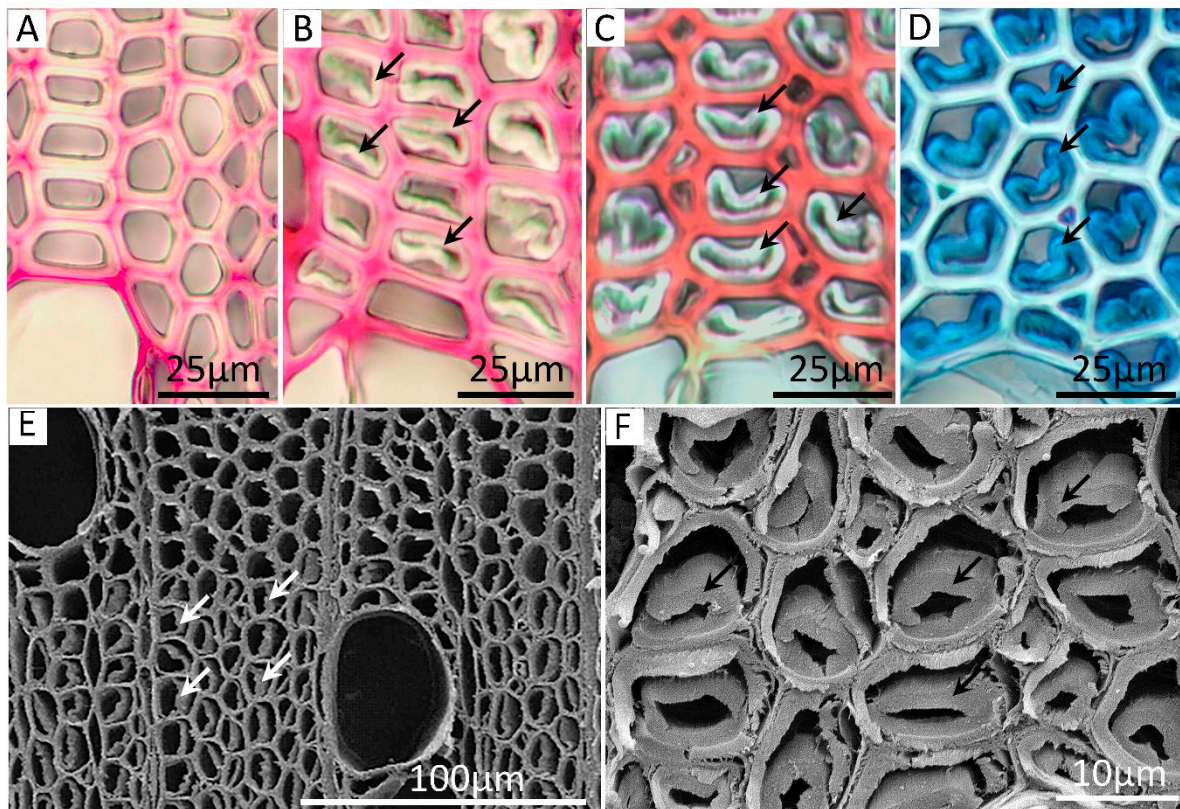


Figure 4. Light microscopy and scanning electron microscopy (SEM) images of typical transverse sections from the *S. viminalis* clones with normal mature and tension wood fibers with a gelatinous layer (arrows); (A,B) normal and tension wood fibers stain pink/red with the Wiesner reaction with vessel cell walls and middle lamellae. There is a weak reaction with the fiber secondary cell walls, and the G-layer is negative (arrows); (C) Mäule reaction with strong orange staining of fiber secondary cell walls and negative reaction with the G-layer; (D) G-fibers after staining with astrablue with detached G-layers; (E,F) SEM images showing thickness of typical G-layers in early- and latewood fibers from the clones. Note, in (E), the upper part of the image shows earlywood fibers without G-layers and the lower part with G-layers.

3.4. Morphometric Analyses of *S. viminalis* Clone Samples

Both the density and wet chemical analysis suggested differences in both the amount and types of biomolecules present, while image analysis of stem sections and histochemistry variations in biopolymer distributions revealed the likely importance of tension wood, G-fibers, and elevated levels of cellulose (i.e., glucose) in certain clone samples. Quantifying tension wood in diverse clone stems is, however, difficult, although recent approaches based on enzymatic hydrolysis and X-ray micro-computed tomography appear promising [35,42]. The purpose here, however, was to explore whether a method based on the characterization of cellular morphological features (particularly for fibers) would be feasible as a characteristic feature. The approach adopted was based on quantifying physical features (e.g., length, width) of 1000 s (minimum 100,000 particles) of cellular elements using an OFA, thereby providing statistical results. Initial analyses were conducted on delignified and macerated fibers of eight *S. viminalis* clone samples selected from the 1172 individuals representing 326 genetically distinct clones. Emphasis was on whether samples of a different size (i.e., stem diameter) could be compared, since fiber length is also known to increase with an increase in stem diameter. Subsequent analyses were performed on two older clones (78183 and 78195) and four commercial *S. viminalis* varieties (Jorr, Olof, Tora, and Björn) with comparable densities (i.e., between 450 and 550 kg/m³; Figure 2B), where comparisons of fiber characteristics were made between whole wood samples and stem regions showing pronounced tension wood; all samples were derived from the basal stem regions (Figure 1).

The OFA gave the results of different classes and the distribution of length-weighted (LW) fiber length vs. proportion of total fiber length in per mille (‰). An analysis of the eight *S. viminalis* clone samples showed slightly skewed normal cumulative distributions with average LW fiber length in the range ca. 0.4–0.5 mm for the eight clones with a maximum LW fiber length of ca. 1.5 mm; results are consistent with published values for young stems (Figure 5). In order to compare the distributions, an appropriate cumulative normal distribution function and Gaussian fit was applied (Figure 6), and the fitted Gaussian curve was characterized by full width half maximum (FWHM), max height, and center of gravity (Table 4). Pearson's correlation was used for revealing correlations between stem diameter and density with LW fiber length distributions (i.e., FWHM, max height, center of gravity). Pearson's correlation analysis showed a significant correlation between stem diameter, density, FWHM, max height, and center of gravity related to the LW fiber length distributions (Table 4, Figure 6).

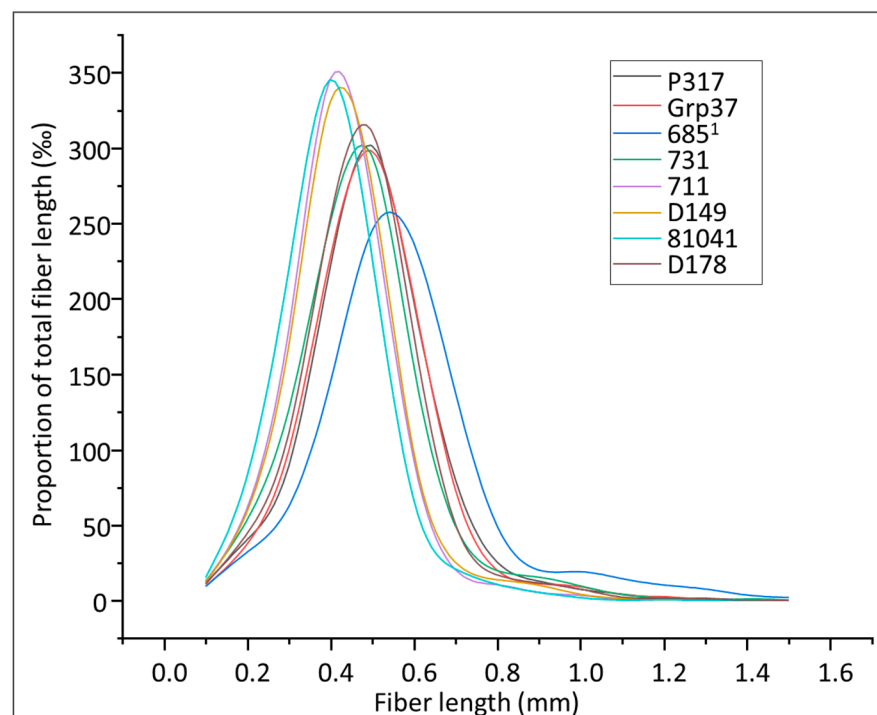


Figure 5. Statistical results of *S. viminalis* clone fiber analysis. 685¹: clone from block 1.

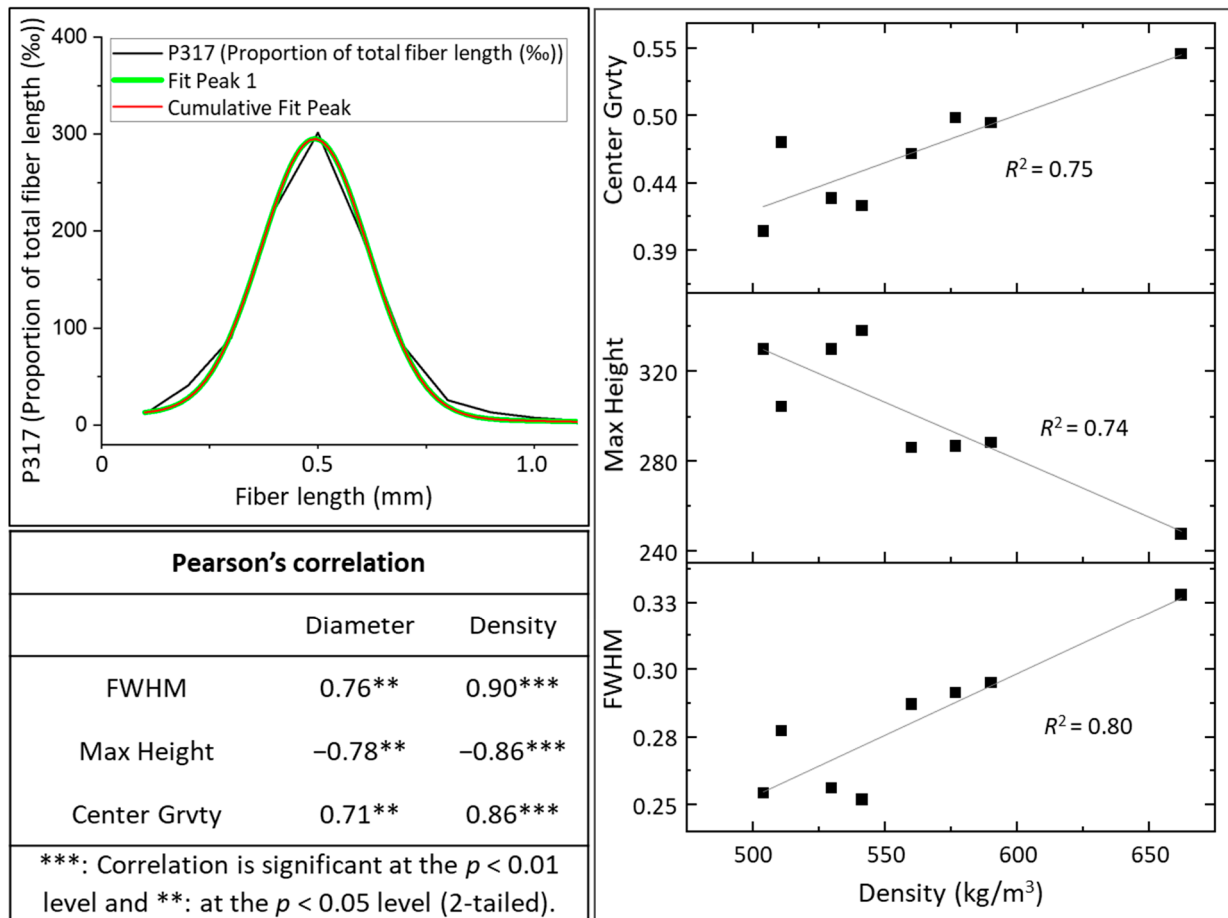


Figure 6. Statistical analysis of fiber characteristics for *S. viminalis* clones. FWHM: full width at half maximum. Center Grvty: center of gravity.

Table 4. Data for Gaussian fit and properties of the *S. viminalis* clones used for statistical analysis.

	FWHM	Max Height	Center Grvty	Diameter (mm)	Density (kg/m ³)
P317	0.29	286.8	0.50	10.3	576.8
Grp37	0.30	288.5	0.49	10.8	590.2
685 ¹	0.33	247.8	0.55	14.9	662.0
731	0.29	286.1	0.46	12.5	560.2
711	0.25	338.4	0.42	8.6	541.3
D149	0.26	330.1	0.43	11.4	529.9
81041	0.25	330.1	0.40	10.2	504.1
D178	0.28	304.4	0.47	12.3	510.9

685¹: clone 685 from block 1; FWHM: full width at half maximum; Center Grvty: center of gravity.

Strong and positive associations were observed between curve-related factors FWHM and center of gravity and stem diameter ($r = 0.76$ and $r = 0.71$, respectively, $p < 0.05$) and stem density ($r = 0.90$ and $r = 0.86$, respectively, $p < 0.01$). Maximum height of the curve showed a strong and negative correlation with stem diameter ($r = 0.78$, $p < 0.05$) and stem density ($r = 0.86$, $p < 0.01$). This indicated that stem density and diameter are significantly related to the LW fiber length's distribution. With *S. viminalis* clone samples showing a relatively smaller stem diameter and lower density (e.g., clone 711), the corresponding LW fiber length's distribution curve has lower FWHM and center of gravity values, but higher max height values. In contrast, in the clone sample with the largest stem diameter with the highest density (i.e., 685¹), the fiber distribution curve had a lower max height, but a higher FWHM value (Figure 5, Table 4). The stem density's Pearson's correlation coefficient value

r was comparatively higher than the diameter (Table 2). Further linear regression analysis was, therefore, performed between stem density and FWHM, max height, and center of gravity. From Figure 6, we note that stem density shows high linear regression values with FWHM, max height, and center of gravity, with R^2 values 0.80, 0.74, and 0.75, respectively. To determine correlations between diameter and fiber distributions, *S. viminalis* samples with similar density values were selected and analyzed using Pearson’s correlation (Figure 7, Table 5). Significant and strong correlations were observed between stem diameter and the LW fiber length distribution curves. Stem diameter showed a positive Pearson’s correlation and linear regression with FWHM and center of gravity with $r = 0.94$, $p < 0.01$, and $r = 0.90$, $p < 0.05$; $R^2 = 0.88$, and 0.82, respectively. In addition, the stem diameter was significant and negatively correlated with max height ($r = 0.95$, $p < 0.01$, $R^2 = 0.89$). These results indicated that stem diameter is significantly related to the LW fiber length’s distribution curve with a similar density value. For using the presence of tension wood in *S. viminalis* clones as a diagnostic feature, similar stem diameter and density should be used.

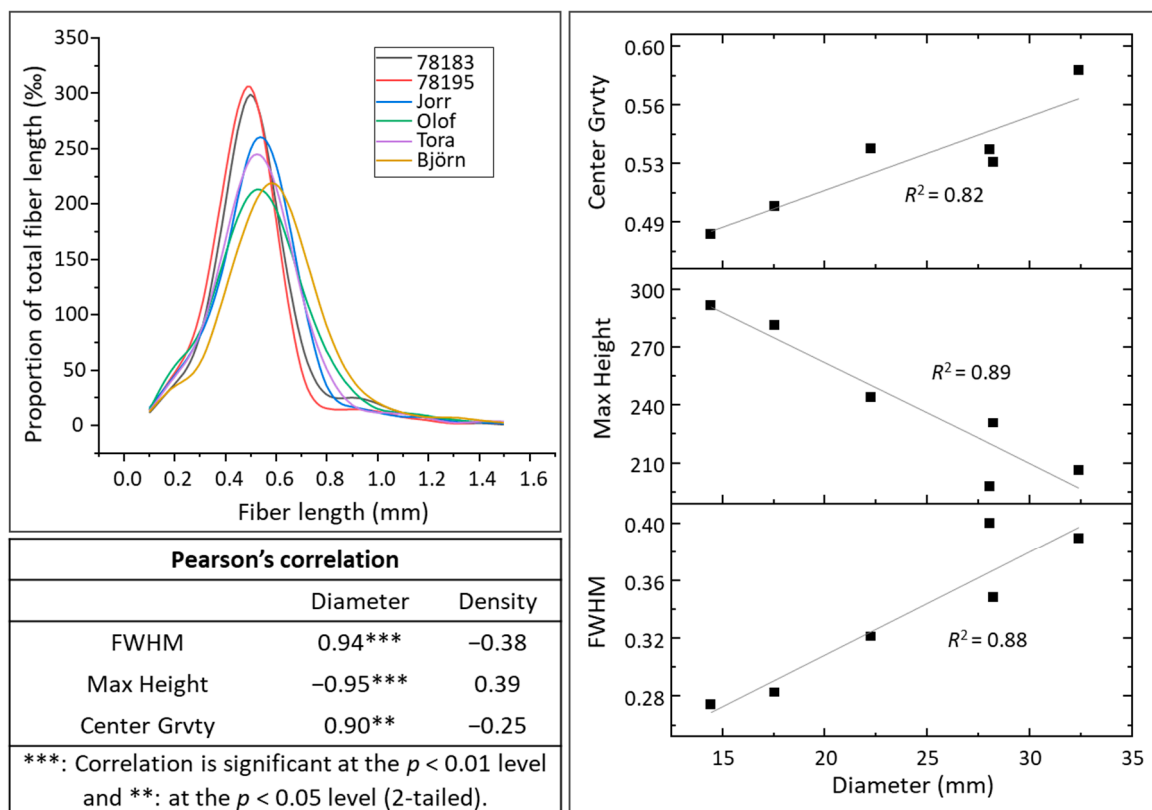


Figure 7. Statistical analysis of fiber characteristics for *S. viminalis* clones and commercial varieties. FWHM: full width at half maximum. Center Grvty: center of gravity.

Table 5. Data for Gaussian fit and properties of the commercial *S. viminalis* clones used for statistical analysis.

	FWHM	Max Height	Center Grvty	Diameter (mm)	Density (kg/m ³)
78183	0.29	281.6	0.50	17.5	506.3
78195	0.27	291.6	0.48	14.4	508.2
Jorr	0.32	244.3	0.53	22.2	508.6
Olof	0.40	197.9	0.53	28.0	499.2
Tora	0.35	230.8	0.53	28.2	459.3
Björn	0.39	206.2	0.58	32.4	493.3

FWHM: full width at half maximum; Center Grvty: center of gravity.

Morphometric analyses performed on five *S. viminalis* samples (from two older clones and three commercial varieties) with similar densities showed variations in LW fiber length cumulative normal distributions between clones and between whole wood samples and tension wood (Figure 8). Tension wood fibers showed comparatively longer fibers in all samples analyzed (Figure 8) indicating that a morphometric approach based on fiber length characteristics may have the potential for distinguishing between clones with and without well-developed tension wood. This was not, however, the case with fiber width distribution where little difference was noted between the different clones when whole wood and tension wood samples were compared (Figure 9). This is not surprising, since in tension wood, the gelatinous layer of fibers contributes to the secondary cell wall thickness independent of the total fiber width.

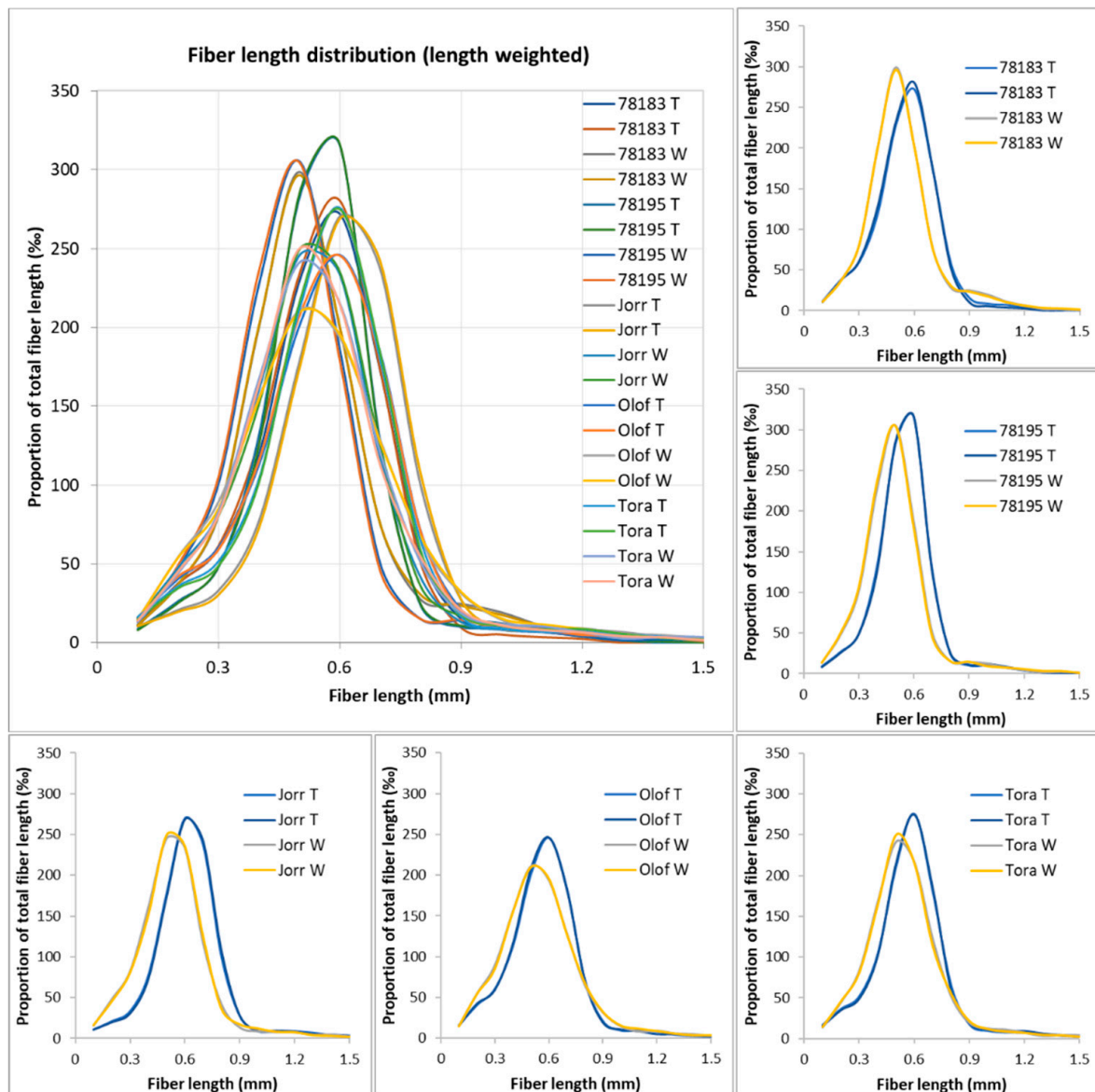


Figure 8. Fiber length distribution (length weighted) of whole and tension wood regions from *S. viminalis* clones and commercial varieties.

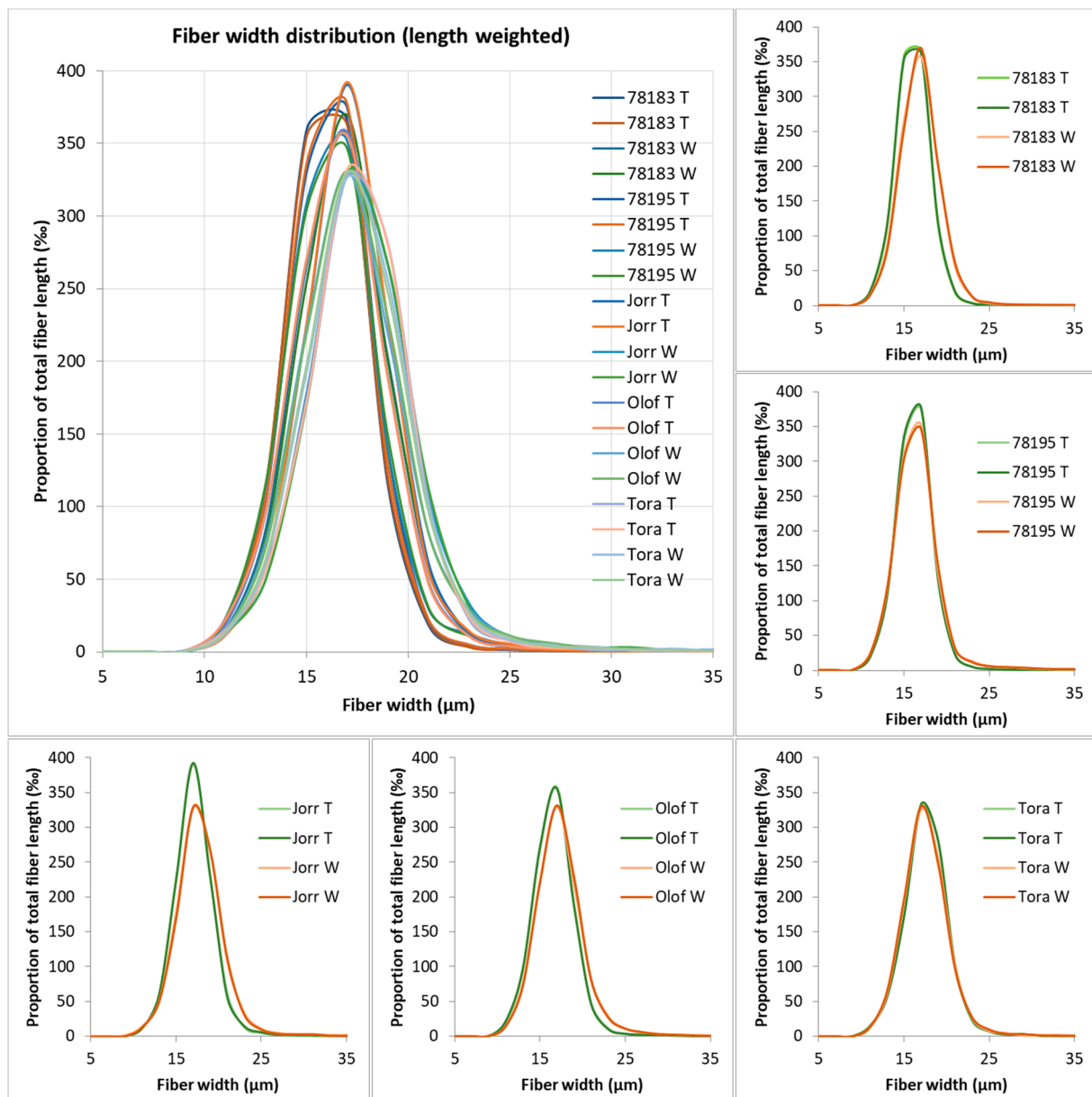


Figure 9. Fiber width distribution (length-weighted) of whole and tension wood regions from *S. viminalis* clones and commercial varieties.

Analysis of vessel frequency as a ratio between OW/TW for six samples (four genetic distinct and three commercial) is shown in Table 6. Results for the frequency of vessels in OW/TW gave ratios between 0.99 (clone 78195) and 3.35 (commercial variety Jorr), indicating similar and lesser numbers of vessels in TW from 100,000 fibers measured. Calculations are based on vessels with a width range of 40–100 μm and length interval of 0.2–0.85 mm (i.e., where over 95% of vessels were found). A comparison between the vessel frequency using OFA (100,000) and SEM counting (ca. 4000 fibers and vessels) for clone 81041 gave ratios of 1.21 and 1.15, respectively, for OW/TW (Table 6), the latter for an area of 0.78×0.89 mm.

Table 6. Ratio of vessels in opposite and tension wood from seven *S. viminalis* clones.

	<i>S. viminalis</i> Samples	Ratio of Vessels in OW and TW
Result from OFA (minimum 100,000 particles)	78183	1.51
	78195	0.99
	Jorr	3.35
	Olof	1.21
	Björn	2.16
	D178	2.59
Observations from SEM (ca. 4000 particles)	81041	1.21
	81041	1.15

(Vessel size: 40–100 μm width, 0.2–0.85 mm length; SEM area: ca. 0.78 \times 0.89 mm).

4. Discussion

Salix is an important coppice plant used through the world as a bioenergy resource [3,43]. Recent interest has, however, been orientated to its potential use as a biomass resource for biofuels as part of the drive towards bioeconomy circularity [7]. An important aspect is, therefore, to find diagnostic markers or traits that are useful for classifying clones of *Salix* as important/interesting for biofuel production. Here, in addition to the yield/hectare and ability to grow on barren ground, more qualifying traits such as density (i.e., biomass volume) and chemistry (i.e., carbohydrate to lignin ratio) are particularly important. For biofuels, beneficial traits should include fast growing attributes with high yield, high cellulose content, and low lignin content. Furthermore, high cellulose content coupled with ease of accessibility for enzymatic hydrolysis is a further important attribute. Accessibility of cellulose in lignocellulose biomass is related to secondary cell wall recalcitrance that is reflected by the total lignin present, type of lignin, and its distribution at different structural (micro-/nanostructural) levels [16,19]. For example, low lignin and hardwood lignin type (i.e., syringyl > guaiacyl lignin) is more favorable for biofuels than low lignin softwoods because of the lignin type [16–18,44]. However, one of the difficulties in characterizing coppice plants such as *Salix* is the great variability that exists, which is under both genotypic and environmental control. Thus, high yields are not only a reflection of good growing conditions but also the inherent gene profile and phenotype expression. Lignocellulose feedstocks from broad plant populations are frequently analyzed for both industrial and scientific purposes by high-throughput screening approaches where entire plant materials are comminuted by chipping and milling to powder. Such approaches have the advantage of achieving rapid results for diversified and large plant populations, and the use of robotics helps the systematic handling and uniformity of sample processing [45]. The downside, however, is that because whole plant materials are processed and only minimal amounts of biomass (i.e., nature of screening process) are analyzed (frequently mgs), the presence of important polymers can be diluted out. In addition, no knowledge is obtained on the distribution of polymers in the native biomass. Since plant materials vary considerably in size, structure, and chemistry with age and to aid comparisons, we applied all our analyses to samples from only *S. viminalis* basal stem regions. Even this approach showed wide variations.

A characteristic feature of the wood anatomy in all (i.e., 20) the basal stem sections of *S. viminalis* clones examined was the presence of tension wood. Tension wood occurred as multilateral and/or unilateral bands in all the basal stem sections examined, present in both growth rings of the two-year-old stems, representing between ca. 6.9 and 39.2% of the total area of the sections (Table 1). These observations are consistent with our previous observations on commercial *S. viminalis* varieties (i.e., Tora, Björn, Loden, and Jorr), where we found tension wood not only formed an important part of sections from basal stem regions but was also present in sections taken at 40 cm points along the entire length of stems [35]. From these observations, we can assume that tension wood is unlikely to be restricted to basal stem regions but is rather an important component of the young rapidly developing *Salix* stems as recorded earlier by Brereton et al. (2012) [29] and Berthod et al. (2015) [14]. Tension wood is normally produced on the upper sides of hardwood species

(e.g., poplar, willow, oak, and birch) [24,25] branches, where it plays a role in maintaining the perpendicular orientation of branches to the axial stem, its induction related to a gravimetric response [24,25]. Enhanced development of tension wood in fast-growing *Salix* stems exposed to adverse strong winds would, however, suggest both gravimetric and genetic differences [14,29]. With several of the genetic clones studied (i.e., 102_PL, 685¹, 81041), the largest areas of tension wood in basal sections were also in agreement with the greatest amount of glucose (i.e., cellulose) and total sugars recorded (Table 1). In one particular example, a *S. viminalis* clone (i.e., 685¹) with relatively large stem diameter and the second highest tension area also showed the highest density, lowest total lignin, next highest glucose, and highest total sugar content suggesting criteria interesting for biofuels (Tables 1 and 2). In several other examples, large tension areas were consistent with high glucose and total sugar and lower lignin levels (Table 1).

The occurrence of tension wood tissues in stems provides elevated cellulose content for plants by developing characteristic G-fibers with cellulose-rich gelatinous layers formed on the lumen side of fiber secondary cell walls [24–27]. Previous studies on the gelatinous layers of a range of hardwoods have shown G-layers to be rich in cellulose, lack lignin, and contain only minor amounts of other carbohydrates and proteins [25]. More recent immunolabelling studies have shown that the gelatinous layer/G-layer secondary wall interface in *S. viminalis* “Astrid” labels strongly for (1-4)- β -D-galactan, mannan, and de-esterified homogalactan [46]. While present studies cannot provide data on the spatial distribution of carbohydrates at the cellular level, both mannose (1.8%–4.0%) and galactose (0.4%–0.9%) were detected in all but one of the clone samples chemically analyzed (Table 1). Total lignin (i.e., acid-insoluble and acid-soluble) in the clones ranged in only 5.6% from 16.4% to 22% (Table 1). Most importantly, however, the gelatinous layers from clones were stained negatively for presence of syringyl (Mäule reaction) and guaiacyl (cinnamaldehydes with Weisner reaction) lignin, the former more pronounced in the outer fiber secondary cell wall and the latter most strongly in vessel and middle lamella regions. A differential spatial distribution of syringyl and guaiacyl lignin in low-lignified hardwoods (e.g., poplar, birch) is common [47], but most importantly, the G-layer appeared non-lignified. The G-layer cellulose should, therefore, not show recalcitrance to enzymatic hydrolysis with cellulases, as we found recently using a commercial cellulase preparation and *Salix* stem sections [35]. Thus, the more tension wood and G-layer present, the more readily available non-recalcitrant cellulose is. This was confirmed by Pearson r (p -value) analysis that showed moderate and strong positive correlations between tension wood, density, and total sugars and negative correlation with lignin Table 2. This means after comminution that *Salix* varieties with high cellulose content, abundant tension wood, and low lignin should have the best biomass attributes for enzymatic hydrolysis and bioethanol production.

While the presence and abundance of tension wood is recognized as an important *Salix* trait for potential bioethanol production, its detection and quantification in stems is, however, difficult. A direct approach using X-ray micro-computed tomography [14] was explored revealing different tissue cell patterning in tension wood, particularly changes in vessel size and distributions compared with normal wood. Gao et al. [35] developed an indirect approach based on enzyme hydrolysis of G-cellulose from stem sections and quantification of the glucose produced in two commercial *S. viminalis* varieties (Björn and Tora), with higher glucose levels indirectly reflecting the greater presence of tension wood.

In the present work, we explored the possibility of using fiber morphometric analysis to determine presence of tension wood in our clones and a number of commercial varieties. The approach is based on using OFA where large quantities of macerated cellular elements (e.g., 100,000 items; fibers, vessels, parenchyma cells) per sample can be measured rapidly and produce statistical results not possible using conventional microscopy approaches. Results were expressed as proportions of total fiber length of length-weighted (LW) fiber length or LW fiber width [48]. The results from fiber analyses of macerated *S. viminalis* wood samples (basal regions) showed differences in LW fiber length proportions in cumulative normal distribution curves from both clones and commercial varieties (Figures 5–7).

However, no apparent difference between clones was observed when LW fiber width was used (Figure 9). Changes in LW fiber length are normal, however, when the stem diameter of plants increase. The results were, therefore, tested using Pearson's correlation analysis. Results showed significant correlations between *S. viminalis* stem diameter, density, and the LW fiber length distributions (Figures 5 and 6). Thus, stem density and diameter were shown as major contributing factors to LW fiber length distributions. Therefore, in order for a legitimate comparison to be made using fiber length as a diagnostic feature for presence of tension wood using an optical analyzer, similar stems, diameters, densities, age, and growing conditions should be used.

We also analyzed LW fiber length, LW fiber width distributions for whole stem samples, and only tension wood regions cut from the same basal stem regions of five clones and commercial varieties (Figures 7 and 8). Results showed differences between genetic clones, but for all matched clone pairs, the LW tension wood fibers were longer (Figure 8). No difference, however, was apparent between the LW width of tension and normal wood fibers (Figure 9). Fiber lengths of TW fibers have been reported as either longer, shorter, or of similar size as normal fibers, with results dependent on wood species [25]. Our results showing the fibers are longer in *S. viminalis* TW compared to non-tension wood fibers are consistent with studies performed on the TW of *Populus euramericana*, a close relative of *S. viminalis* [49]. A further possibility for detecting TW used in this study was the frequency of vessels. While hardwoods in general show variations in vessel frequency and proportion, studies have shown a reduction in vessel diameter and frequency in TW compared with non-tension wood [49,50]. For example, Jourez et al. [49] reported that the vessel frequency and area of vessel lumen was lower in tension wood of *Poplar* spp., while Brereton et al. [29] using X-ray microcomputer tomography found that the frequency of vessels was reduced in *S. viminalis*, although the total vessel volume was increased. A similar trend was observed in present studies where the ratio of *S. viminalis* OW/TW showed a reduction in vessel frequency in TW using OFA and SEM approaches. Thus, together with fiber length, vessel frequency may provide a complementary trait to be used as a diagnostic feature for determining TW in fast growing *S. viminalis*.

In summary, a morphometric approach using an optical analyzer for distinguishing tension wood fibers and normal wood fibers in *S. viminalis* clones has potential for use as a diagnostic feature. Differences in vessel frequency distributions were also noted between tension wood and whole wood samples as previously reported in *S. viminalis* stems [14] and differences with opposite wood. In tension wood, the vessels tended to be longer compared to normal wood. A diagnostic feature that has even greater potential than either fiber length and vessel size and distribution for distinguishing between tension wood and normal wood fibers is fiber cell wall thickness. As shown during the present study, the average width of both tension and normal wood fibers is similar (ca. 16–19 μm ; Figure 9), while the difference in fiber cell wall thickness in both earlywood and latewood fibers can be large (Figure 4) and in the order of 2–3 \times because of the thickness of the G-layer (Figure 4).

5. Conclusions

A systematic investigation was performed on a population (326) of genetically distinct clones and commercial *S. viminalis* using complementing approaches (density, microscopy, chemical, image, morphometric, and statistical analyses) to determine interesting traits for biofuel potential. Similar basal regions from all clones were used to aid comparisons. Results showed considerable variability between genetic clones based on density (i.e., ca. 300–660 kg/m^3) and chemistry, while image analysis and microscopy confirmed the presence of tension wood as an important tissue component in all clones including commercial varieties. Tension wood formed multilateral/unilateral bands in varying amounts in all clone basal stem sections examined. Tension wood fibers showed characteristic non-lignified gelatinous layers of various thickness. Several clones selected for in-depth chemical and subsequent image analysis showed high glucose (i.e., cellulose) to correspond with the presence of pronounced tension wood and certain clones with the highest lignin

had a lower percentage of tension wood. Complementary morphometric and statistical analyses showed that tension wood fibers could be distinguished from normal wood fibers by length, but not width in stems of similar density and diameter using optical fiber analyses. Similarly, differences in vessel frequency and length were demonstrated between tension and opposite wood. Since tension wood is reported in other *Salix* species [51] and widely reported in Poplar [25], a closely related plant species, it can be regarded as a common and important trait. As tension wood can provide elevated levels of not only structural cellulose (i.e., located in the cell walls) but rather recalcitrant-free cellulose (i.e., cellulose lacks lignin encapsulation), it would be highly desirable for *Salix* breeding programs to examine the possibilities of using recurrent vegetative selection of this trait as a marker. Possibly, this can be used together using genome-wide (GWAS) association studies. A problem still exists in detecting the presence of tension wood in *Salix* stems in plantations. However, morphometric analysis—although destructive—of macerated wood samples offers a possible step forward where very large populations of fiber/vessel elements can be analyzed rapidly, providing a quantitative reference allowing for a database to be built up.

Author Contributions: Conceptualization: G.D., J.G., N.T. and M.J.; methodology: J.G., G.D., M.J. and N.T.; writing G.D. and J.G.; review editing: G.D., J.G. All authors have read and agreed to the published version of the manuscript.

Funding: This study was performed within the research projects OPTUS and Biomaterial nanostructure that are financed by the Swedish Research Council for Environmental, Agricultural Sciences and Spatial Planning (Formas) under Project Numbers 2016-20031 and 2018-00997.

Acknowledgments: The authors thank Associate Professor Ann Christin Rönnberg-Wästljung from the Department of Plant Biology and Professor Martin Weih and Nils-Erik Nordh from the Department of Crop and Production Ecology for interesting discussions and making available *S. viminalis* variants and field study information.

Conflicts of Interest: The authors declare no conflict of interest.

References

1. Pu, Y.; Zhang, D.; Singh, P.M.; Ragauskas, A.J. The new forestry biofuels sector. *Biofuels Bioprod. Bioref.* **2008**, *2*, 58–73. [[CrossRef](#)]
2. Karp, A. Willows as a source of renewable fuels and diverse products. In *Challenges and Opportunities for the World's Forests in the 21st Century*; Springer: Berlin, Germany, 2014; pp. 617–641.
3. Sassner, P.; Galbe, M.; Zacchi, G. Techno-economic evaluation of bioethanol production from three different lignocellulosic materials. *Biomass Bioenergy* **2008**, *32*, 422–430. [[CrossRef](#)]
4. Serapiglia, M.J.; Cameron, K.D.; Stipanovic, A.J.; Abrahamson, L.P.; Volk, T.; Smart, L.B. Yield and woody biomass traits of novel shrub willow hybrids at two contrasting sites. *Bioenergy Res.* **2013**, *6*, 533–546. [[CrossRef](#)]
5. Pawar, P.M.-A.; Schnürer, A.; Mellerowicz, E.J.; Rönnberg-Wästljung, A.C. QTL mapping of wood FT-IR chemotypes shows promise for improving biofuel potential in short rotation coppice willow (*Salix* spp.). *Bioenergy Res.* **2018**, *11*, 351–363. [[CrossRef](#)]
6. Horn, S.J.; Estevez, M.M.; Nielsen, H.K.; Linjordet, R.; Eijsink, V.G. Biogas production and saccharification of *Salix* pretreated at different steam explosion conditions. *Bioresour. Technol.* **2011**, *102*, 7932–7936. [[CrossRef](#)]
7. Weih, M.; Hansson, P.A.; Ohlsson, J.A.; Sandgren, M.; Schnürer, A.; Rönnberg Wästljung, A. Sustainable production of willow for biofuel use. In *Achieving Carbon-Negative Bioenergy Systems from Plant Materials*; Saffron, C., Ed.; Burleigh Dodds Science Publishing Limited: Cambridge, UK, 2020; pp. 1–36.
8. Materials Economics, M. *EU Biomass Use in a Net-Zero Economy—A Course Correction for EU Biomass*; Material Economic Sverige AB: Stockholm, Sweden, 2021.
9. Stolarski, M.J.; Szczukowski, S.; Tworkowski, J.; Klasa, A. Yield, energy parameters and chemical composition of short-rotation willow biomass. *Ind. Crop. Prod.* **2013**, *46*, 60–65. [[CrossRef](#)]
10. Hallingbäck, H.R.; Berlin, S.; Nordh, N.-E.; Weih, M.; Rönnberg-Wästljung, A.-C. Genome wide associations of growth, phenology, and plasticity traits in willow [*Salix viminalis* (L.)]. *Front. Plant Sci.* **2019**, *10*, 753. [[CrossRef](#)]
11. Karp, A.; Hanley, S.; Trybush, S.O.; Macalpine, W.; Pei, M.; Shield, I. Genetic improvement of willow for bioenergy and biofuels free access. *J. Integr. Plant Biol.* **2011**, *53*, 151–165. [[CrossRef](#)]
12. Berlin, S.; Trybush, S.O.; Fogelqvist, J.; Gyllenstrand, N.; Hallingbäck, H.R.; Åhman, I.; Nordh, N.-E.; Shield, I.; Powers, S.J.; Weih, M.; et al. Genetic diversity, population structure and phenotypic variation in European *Salix viminalis* L. (Salicaceae). *Tree Genet. Genomes* **2014**, *10*, 1595–1610. [[CrossRef](#)]
13. Ray, M.J.; Brereton, N.J.B.; Shield, I.; Karp, A.; Murphy, R.J. Variation in cell wall composition and accessibility in relation to biofuel potential of short rotation coppice willows. *Bioenergy Res.* **2012**, *5*, 685–698. [[CrossRef](#)]

14. Berthod, N.; Brereton, N.J.B.; Pitre, F.E.; Labrecque, M. Five willow varieties cultivated across diverse field environments reveal stem density variation associated with high tension wood abundance. *Front. Plant Sci.* **2015**, *6*, 948. [[CrossRef](#)] [[PubMed](#)]
15. Pilate, G.; Guiney, E.; Holt, K.; Petit-Conil, M.; Lapierre, C.; Leple, J.-C.; Pollet, B.; Mila, I.; Webster, E.A.; Marstorp, H.G.; et al. Field and pulping performances of transgenic trees with altered lignification. *Nat. Biotechnol.* **2002**, *20*, 607–612. [[CrossRef](#)]
16. Himmel, M.E.; Ding, S.-Y.; Johnson, D.K.; Adney, W.S.; Nimlos, M.R.; Brady, J.W.; Foust, T.D. Biomass recalcitrance: Engineering plants and enzymes for biofuels production. *Science* **2007**, *315*, 804–807. [[CrossRef](#)]
17. Davison, B.H.; Drescher, S.R.; Tuskan, G.; Davis, M.; Nghiem, N.P. Variation of S/G ratio and lignin content in a *Populus* family influences the release of xylose by dilute acid hydrolysis. *Appl. Biochem. Biotechnol.* **2006**, *130*, 427–435. [[CrossRef](#)]
18. Chen, F.; Dixon, R.A. Lignin modification improves fermentable sugar yields for biofuel production. *Nat. Biotechnol.* **2007**, *25*, 759–761. [[CrossRef](#)]
19. Chundawat, S.; Donohoe, B.S.; Sousa, L.D.C.; Elder, T.; Agarwal, U.P.; Lu, F.; Ralph, J.; Himmel, M.E.; Balan, V.; Dale, B.E. Multi-scale visualization and characterization of lignocellulosic plant cell wall deconstruction during thermochemical pretreatment. *Energy Environ. Sci.* **2011**, *4*, 973–984. [[CrossRef](#)]
20. Anderson, N.A.; Tobimatsu, Y.; Ciesielski, P.N.; Ximenes, E.; Ralph, J.; Donohoe, B.S.; Ladisch, M.; Chapple, C. Manipulation of guaiacyl and syringyl monomer biosynthesis in an *Arabidopsis* cinnamyl alcohol dehydrogenase mutant results in atypical lignin biosynthesis and modified cell wall structure. *Plant Cell* **2015**, *27*, 2195–2209. [[CrossRef](#)]
21. Lockhart, J. Altering lignin composition to improve biofuel production. *Plant Cell* **2015**, *27*, 2082. [[CrossRef](#)]
22. McCann, M.C.; Carpita, N.C. Biomass recalcitrance: A multi-scale, multi-factor, and conversion-specific property. *J. Exp. Bot.* **2015**, *66*, 4109–4118. [[CrossRef](#)]
23. Serapiglia, M.J.; Humiston, M.C.; Xu, H.; Hogsett, D.A.; De Orduña, R.M.; Stipanovic, A.J.; Smart, L.B.S. Enzymatic saccharification of shrub willow genotypes with differing biomass composition for biofuel production. *Front. Plant Sci.* **2013**, *4*, 57. [[CrossRef](#)]
24. Ruelle, J. Morphology, anatomy and ultrastructure of reaction wood. In *The Biology of Reaction Wood*; Springer: Berlin, Germany, 2014; pp. 13–35.
25. Gardiner, B.; Barnett, J.; Saranpää, P.; Gril, J. *The Biology of Reaction Wood*; Springer: Berlin, Germany, 2014.
26. Daniel, G.; Filonova, L.; Kallas, Å.M.; Teeri, T.T. Morphological and chemical characterisation of the G-layer in tension wood fibres of *Populus tremula* and *Betula verrucosa*: Labelling with cellulose-binding module CBM1_{HjCel7A} and fluorescence and FE-SEM microscopy. *Holzforschung* **2006**, *60*, 618–624. [[CrossRef](#)]
27. Lehringer, C.; Daniel, G.; Schmitt, U. TEM/FE-SEM studies on tension wood fibres of *Acer* spp., *Fagus sylvatica* L. and *Quercus robur* L. *Wood Sci. Technol.* **2009**, *43*, 691–702. [[CrossRef](#)]
28. Foston, M.; Hubbell, C.A.; Samuel, R.; Jung, S.; Fan, H.; Ding, S.-Y.; Zeng, Y.; Jawdy, S.; Davis, M.; Sykes, R.; et al. Chemical, ultrastructural and supramolecular analysis of tension wood in *Populus tremula* × *alba* as a model substrate for reduced recalcitrance. *Energy Environ. Sci.* **2011**, *4*, 4962–4971. [[CrossRef](#)]
29. Brereton, N.J.; Ray, M.J.; Shield, I.; Martin, P.; Karp, A.; Murphy, R.J. Reaction wood—a key cause of variation in cell wall recalcitrance in willow. *Biotechnol. Biofuels* **2012**, *5*, 1–11. [[CrossRef](#)]
30. Larsson, S. Genetic improvement of willow for short-rotation coppice. *Biomass Bioenergy* **1998**, *15*, 23–26. [[CrossRef](#)]
31. Ohlsson, J.A.; Hallingbäck, H.R.; Jebrane, M.; Harman-Ware, A.E.; Shollenberger, T.; Decker, S.R.; Sandgren, M.; Rönnerberg-Wästljung, A.-C. Genetic variation of biomass recalcitrance in a natural *Salix viminalis* (L.) population. *Biotechnol. Biofuels* **2019**, *12*, 1–12. [[CrossRef](#)]
32. Stamm, A.J. Density of wood substance, adsorption by wood, and permeability of wood. *J. Phys. Chem.* **1929**, *33*, 398–414. [[CrossRef](#)]
33. Sluiter, A.; Hames, B.; Ruiz, R.; Scarlata, C.; Sluiter, J.; Templeton, D.; Crocker, D.L.A.P. Determination of structural carbohydrates and lignin in biomass. *Lab. Anal. Proced.* **2012**, *1617*, 1–15.
34. Robards, A.W.; Purvis, M.J. Chlorazol black E as a stain for tension wood. *Stain Technol.* **1964**, *39*, 309–315. [[CrossRef](#)]
35. Gao, J.; Jebrane, M.; Terziev, N.; Daniel, G. Enzymatic hydrolysis of the gelatinous layer in tension wood of *Salix* varieties as a measure of accessible cellulose for biofuels. *Biotechnol. Biofuels* **2021**, *14*, 1–18. [[CrossRef](#)]
36. Nakagawa, K.; Yoshinaga, A.; Takabe, K. Anatomy and lignin distribution in reaction phloem fibres of several Japanese hardwoods. *Ann. Bot.* **2012**, *110*, 897–904. [[CrossRef](#)]
37. Kim, J.S.; Gao, J.; Terziev, N.; Cuccui, I.; Daniel, G. Chemical and ultrastructural changes of ash wood thermally modified using the thermo-vacuum process: I. Histo/cytochemical studies on changes in the structure and lignin chemistry. *Holzforschung* **2015**, *69*, 603–613. [[CrossRef](#)]
38. Daniel, G. Microscope techniques for understanding wood cell structure and biodegradation. In *Secondary Xylem Biology*; Elsevier: Amsterdam, The Netherlands, 2016; pp. 309–343.
39. Wise, L.E. Chlorite holocellulose, its fractionation and bearing on summative wood analysis and on studies on the hemicelluloses. *Pap. Trade* **1946**, *122*, 35–43.
40. Klačnja, B.; Orlović, S.; Galić, Z. Comparison of different wood species as raw materials for bioenergy. *South-East Eur. For. SEEFOR* **2013**, *4*, 81–88. [[CrossRef](#)]
41. Clair, B.; Thibaut, B.; Sugiyama, J. On the detachment of the gelatinous layer in tension wood fiber. *J. Wood Sci.* **2005**, *51*, 218–221. [[CrossRef](#)]

42. Brereton, N.J.B.; Ahmed, F.; Sykes, D.; Ray, M.J.; Shield, I.; Karp, A.; Murphy, R.J. X-ray micro-computed tomography in willow reveals tissue patterning of reaction wood and delay in programmed cell death. *BMC Plant Biol.* **2015**, *15*, 1–12. [[CrossRef](#)]
43. Ledin, S. Willow wood properties, production and economy. *Biomass Bioenergy* **1996**, *11*, 75–83. [[CrossRef](#)]
44. Jeoh, T.; Ishizawa, C.I.; Davis, M.; Himmel, M.E.; Adney, W.S.; Johnson, D.K. Cellulase digestibility of pretreated biomass is limited by cellulose accessibility. *Biotechnol. Bioeng.* **2007**, *98*, 112–122. [[CrossRef](#)]
45. Ohlsson, J.A.; Harman-Ware, A.E.; Sandgren, M.; Schnürer, A. Biomass recalcitrance in willow under two biological conversion paradigms: Enzymatic hydrolysis and anaerobic digestion. *Bioenergy Res.* **2020**, *13*, 260–270. [[CrossRef](#)]
46. Gritsch, C.; Wan, Y.; Mitchell, R.A.C.; Shewry, P.R.; Hanley, S.J.; Karp, A. G-fibre cell wall development in willow stems during tension wood induction. *J. Exp. Bot.* **2015**, *66*, 6447–6459. [[CrossRef](#)]
47. Obst, J.R. Lignins: Structure and distribution in wood and pulp. *MRS Online Proc. Libr.* **1990**, *197*, 11–20. [[CrossRef](#)]
48. Ai, J.; Tschirner, U. Fiber length and pulping characteristics of switchgrass, alfalfa stems, hybrid poplar and willow biomasses. *Bioresour. Technol.* **2010**, *101*, 215–221. [[CrossRef](#)]
49. Jourez, B.; Riboux, A.; Leclercq, A. Anatomical characteristics of tension wood and opposite wood in young inclined stems of poplar (*Populus euramericana* cv ‘Ghoy’). *IAWA J.* **2001**, *22*, 133–157. [[CrossRef](#)]
50. Clair, B.; Ruelle, J.; Beauchêne, J.; Prévost, M.F.; Fournier, M. Tension wood and opposite wood in 21 tropical rain forest species. *IAWA J.* **2006**, *27*, 341–376. [[CrossRef](#)]
51. Xu, F.; Sun, R.-C.; Lu, Q.; Jones, G.L. Comparative study of anatomy and lignin distribution in normal and tension wood of *Salix gordejecii*. *Wood Sci. Technol.* **2006**, *40*, 358. [[CrossRef](#)]